MARAAL: A Low Altitude Long Endurance Solar Powered UAV for Surveillance and Mapping Applications ⋆

Vijay Shankar Dwivedi * **Jay Patrikar** * **Amulya Addamane** *
A. K. Ghosh *

* *Department of Aerospace Engineering,Indian Institute of Technology Kanpur, Kanpur, UP 208016, India*
e-mail: {vijayd|jaypat|amulya|akg} @iitk.ac.in

Abstract: This paper constitutes the detailed design, fabrication and flight tests of MARAAL: A low altitude long endurance UAV to be operated day-night in a subtropical region.The Solar UAV prototype fabricated at Unmanned Aerial Laboratory IIT Kanpur has a wing span of 5.35m, maximum endurance of 16 hours and a maximum payload capacity of 6 kgs.A detailed conceptual design process is established with a set of constraints which are used to generate parameters for 6DOF simulation. Developments in solar cell encapsulation process ensure a superior aerodynamic performance. The paper also highlights the construction efforts and details of the hardware and onboard electronics including surveillance equipment.

Keywords: Solar energy,Solar cells, Automated guided vehicles, Computer-aided design,Energy management systems,mobile robots

1. INTRODUCTION

Recently, Unmanned Aerial Vehicles or UAVs are increasingly being used in both military and civilian applications. They can provide safety and comfort in jobs that earlier required the presence of a human pilot. From domains such as precision agriculture, remote sensing and environmental monitoring to disaster relief operations, as seen in works by Zhang and Kovacs (2012), Berni et al. (2009), Dunbabin and Marques (2012), and Goodrich et al. (2008), UAVs have proven to be exceedingly useful. However, accompanying this increasing use is also a natural drive to make the systems more flexible and robust in terms of their capabilities including endurance and large power reserves.

In comparison to rotary based UAVs which generate lift using a set of blades, fixed wing UAVs that generate lift using wings are known to have more endurance as majority of the power is consumed in only overcoming drag. Thus, fixed wing aircraft are more efficient and can carry larger payloads as opposed to rotary aircrafts. But there still exists a limit on the endurance because of the fixed energy reserves that it carries in form of batteries/fuel. That is why technology is currently being developed to harness energy while the aircraft is in flight. One of the front runners is the use of solar energy to power an aircraft. A carefully designed aircraft with suitable environmental conditions can exhibit long-endurance capability, especially in the extreme form of continuous multi-day flight, or perpetual endurance as conveyed by Oettershagen et al. (2015).

We have come a long way from the first flight of a solar powered aircraft by Colella and Wenneker (1996), to the relatively recent round-the-world attempt by Team Solar Impulse(see Ross (2008)) in a 72m wingspan, 2300kg aircraft. However, although a lot of work has been done in large wingspan (above 20m) High-Altitude-Long-Endurance (HALE) class of solar powered aircrafts as detailed by Sai et al. (2017), a lot more still needs to be done in Low-Altitude Long-Endurance (LALE) class. Notable attempts include the SoLong by Cocconi (2005) which performed a 48-hour continuous flight while seeking updrafts, the 3.2m wingspan Sky-Sailor by Noth et al. (2008) which performed 27-hour long flight using updrafts and recently the AtlantikSolar, a 5.6m-wingspan UAV developed for Search and Rescue (SAR) missions by Oettershagen et al. (2015).

Fig. 1. SUAV MARAAL prototype with a wingspan of 5.35m developed at the UAV Lab at IIT Kanpur.

⋆ This work was supported by Aeronautics Research and Development Board (ARDB), Banglore

This paper details the research that is currently being undertaken at the UAV Laboratory in IIT Kanpur in designing and fabricating a LALE-UAV solar powered platform as shown in Fig. 1. The goals of the project have been identified as

(1) Maximum takeoff weight should be less than 20kg
(2) A payload capacity of 5kg to 10 kg: The payload can be a stabilized infrared camera used for the surveillance purposes or instruments for applications in communication relay.
(3) Endurance greater than 15 hours: In order to further increase the endurance, solar cells will be installed on various UAV surfaces as per power needed.
(4) Operating altitude of 1 to 5 km above the ground in order to cover maximum area during reconnaissance.

The paper has been divided as follows: Sec. 2 details the various design constraints and mathematical models to simulate them and Sec. 3 shows the design methodology based on those constraints. Sec. 4 explains the construction techniques and on-board architectures used to realize a prototype of the model whose preliminary flight test results are shown in Sec. 5.

2. STUDY OF CONSTRAINTS

Any detailed study involves a set of constraints which are often imposed by the environment in which the system operates and also by state of the art essential technology components.

2.1 Solar Irradiance

The performance of a solar powered UAV depends to a large extent on how well the system is designed to take advantage of the available solar power. It thus becomes important to study the solar radiance that is available in Kanpur ($26.449923N$, $80.331874E$), which is the location of operations. Algorithm 1 is used to calculate the power available from the sun and is based on earlier work done by Duffie and Beckman (2013). Note that the solar constant (G_{sc})is the energy obtained from the sun on a unit area surface perpendicular to the direction of propagation of the radiation at mean earth-sun distance (1 AU) outside the atmosphere. We use the method by Hottel (1976), which takes into account zenith angle and altitude, for estimating the beam radiation transmitted through clear atmosphere. Next, in order to compute the amount of total energy incident on the solar panel daily, we integrate the hourly solar irradiance and obtain the daily solar irradiation H_o in joules per square meter per day. This solar irradiation does not take atmosphere in consideration, which is assumed to be absent. Angstrom-type regression equation now relates monthly average daily radiation to clear-day radiation at the location and the average fraction of possible sunshine hours. Various sets of constants a and b for various locations and climate types have been developed based on solar radiation data available. Seeing the table in Duffie and Beckman (2013), we find the climate and vegetation of Kanpur to be comparable with that of Brownsville, Texas, i.e., Steppe or semi-arid climate and Broadleaf deciduous, shrub form vegetation. Using these values, daily average power during daytime is calculated as

Algorithm 1 Algorithm to calculate the avg Irradiance

$G_{sc} = 1367W/m^2$ ▷ Solar Constant
$\Phi = 26.5°$ ▷ Latitude of Kanpur
a = 0.31
b = 0.35 ▷ Empirical constants
for `n=1 to 365` **do** ▷ nth day of the year
  for θ_z=$-90°$ to $90°$ **do** ▷ Sun zenith angle
    $G_o = G_{sc}\big(1 + 0.033cos(\frac{360n}{365})\big)$
      ▷ Radiation incident on normal plane
    $\delta = 23.45sin(360\frac{284+n}{365})$ ▷ Solar Declination
    $cos(\omega) = -tan(\Phi)tan(\delta)$ ▷ Hour angle
    $N = \frac{2}{15}\omega$ ▷ Number of daylight hours
    $a_o = 0.95(0.4237 - 0.00821(6 - A)^2)$
      ▷ A=Altitude of the UAV(km)
    $a_1 = 0.98(0.5055 - 0.00595(6.5 - A)^2)$
    $k = 1.02(0.2711 - 0.01858(2.5 - A)^2)$
    $\tau_b = a_o + a_1 e^{\frac{-k}{cos\theta_z}}$
      ▷ Atmospheric transmittance
    $G_{cb} = \tau_b G_o cos\theta_z$ ▷ Clear sky beam radiation
    $\tau_d = 0.271 - 0.294\tau_b$ ▷ Atmospheric diffusion
    $G_d = \tau_d G_o$ ▷ Diffused radiation
    $G_{radiation_n} = G_{cb} + G_d$ ▷ Total radiation
  end for ▷ Integrate for a day
  $H_o = \frac{86400G_{rad}}{\pi}(cos\Phi cos\delta sin\omega + \frac{\pi\omega}{180}sin\Phi sin\delta)$
    ▷ Daily avg extraterrestrial solar irradiation
  $\frac{H}{H_o} = a + b\frac{n}{N}$
    ▷ Daily average solar irradiation
end for

$$P_{avg} = \frac{H}{3600 \times N} \tag{1}$$

2.2 Solar cells

The main objective here is only to give a short and non-exhaustive overview of the existing types and select a solar cell which will be used in our UAV. Solar cells, also known as photovoltaic cells, are device that convert solar energy into electrical energy using the photovoltaic effect. Because they provide a clean and long-duration source of energy and require almost no maintenance, they are widely used in space applications. They are composed of one or multiple layers of semiconducting materials such as Silicon which is mostly being used because it is cheap and second most abundant element in Earths crust. The silicon solar cells can be distinguished according to the type of crystal: Monocrystalline, Polycrystalline, and Amorphous. Other materials like elements from groups three to five of the Periodic Table of the elements are also used to produce compound solar cells. These include gallium arsenide (GaAs), copper indium diselenide (CIS), Copper indium gallium selenide (CIGS), cadmium telluride (CdTe), etc. These cells are very expensive to produce, but have higher efficiency. Organic photovoltaics also need to be mentioned. The polymer solar cells made up of organic material and the dye sensitized solar cells that are very promising technologies because their fabrication costs are very inexpensive. However, the above technologies suffer from unstable efficiency problems that still must be solved and are therefore not yet viable for industry.

I-V Characteristic The solar cells have a very characteristic current to voltage curve shape. When the cell

Solar cell	Length	Breadth	Thickness	Voc	Isc	Vmp	Imp	Power	Efficiency
Sun Power A300	125.0	125.0	0.3	0.7	5.9	0.6	5.5	3.1	21.5
RC7.2-75 Flex solar cell	270	90.0	0.2	10.5	0.1	7.2	0.1	0.7	3.0
Wave sol Ascent Solar 1.1	1148	330	NA	23.0	1.9	15.8	1.4	21.0	5.5
NanosolarNanoCell 26 Watts	165.0	135.0	0.4	0.6	6.7	0.5	5.8	2.6	11.7
DIY 0.5W2V/ 330MA	194.0	60.0	NA	1.5	0.3	NA	NA	0.5	4.3
Sun power C60	125.0	125.0	0.2	0.7	6.3	0.6	5.9	3.4	22.5
IXOLARTM High Efficiency SolarBIT.	22.0	7.0	1.8	0.6	0.1	0.5	0.0	0.0	22.0
Spectro Lab	80.0	40.0	0.1	2.7	0.5	2.4	0.5	1.2	28.3

Table 1. Solar Cell Market Analysis

pads are not connected, no current is produced and the voltage equals the open circuit voltage. When the cell is short circuited, the voltage is zero but the current equals short circuit current. At these two extreme points(both cases), the power retrieved is zero. In between, there is a working point, called the maximum power point, where the power one can retrieve is the highest. Cells should be operating precisely at this point. However, the curve, and thus this point, is not fixed and varies depending on many parameters. A Maximum Power Point Tracker(MPPT) is used to exploit this characteristic.

Panels To increase the current, solar cells are arranged in parallel and to increase the voltage, they are connected in series. This arrangement is referred to as a solar module or solar panel. The I-V curve of a solar panel has a scaled but similar shape to that of the single solar cell curve.

Market study Efficiency, size, cost and weight are few important parameters considered in selecting the most suitable solar cells for the solar UAV. Flexibility in the solar cells is also desired in order to place them at non-flat surfaces. Most of the solar cells available in the market weigh a lot and are meant for household, roof tops purposes. They also have low efficiency and low cost. Some others, though lightweight and have high efficiency, are bit costly. Table 1 compares some available cells. Even though Spectrolabs solar cell has the highest efficiency, we will prefer Sun Power Maxion C60 because they are less expensive, have decent efficiency, and available in small size which will help us to place the solar cells on the wing and other curved surfaces without affecting much of the geometry.

3. CONCEPTUAL DESIGN

While designing a solar UAV that operates for extended periods of time, a critical parameter is to strike a balance between the amount of energy received from the solar panels and the energy required by the system. The design analysis in this paper relies mostly on the integrated model with dependent integration given by Wilkins et al. (2009) with a few changes tailored to the goals as mentioned in section 1.

3.1 Energy model

The power generated by the solar cells is given by

$$P_{gen} = \eta_{solar} \times \eta_{mppt} \times \eta_{area} \times S \times G$$

where η_{solar} is the solar cell efficiency, η_{mppt} is the efficiency associated with the MPPT, S is the wing area, G is the Solar irradiance in $[W/m^2]$, P_{gen} is the Electrical

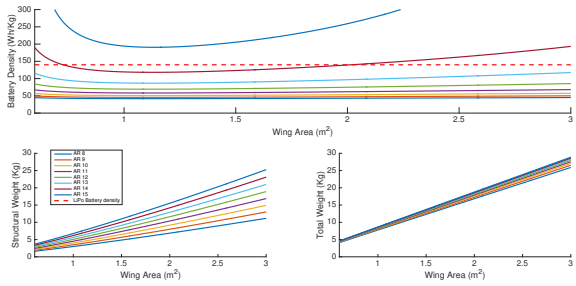

Fig. 2. Design Conceptualization

power provided by solar cells and η_{area} is the percentage of wing area covered by solar cells which also accounts for solar cells installed on horizontal stabilizer. Most of the solar design analysis in literature take into account only the constant altitude loiter flights. However in general, the solar energy in an aircraft can be stored in two forms: in the form of chemical energy stored in the batteries and in form of potential energy of the height gained by the aircraft. This consideration becomes important especially in cases when there is a constraint on how fast the system can charge batteries. Thus the energy consumption equation under the assumption of unaccelerated flight becomes

$$P_{req} = P_{drag} + W\frac{dh}{dt} + P_{avionics}$$

where using estimated value of $P_{avionics}$ and assuming $\frac{dh}{dt} << V$, where V is the airspeed corresponding to minimum energy consumption(hence minimum power) which the UAV is assumed to fly at, we can calculate the corresponding maximum weight of the UAV using (2) for level flight

$$W = \left(P_{drag}\sqrt{\frac{\rho S}{2}}\frac{C_L^{3/2}}{C_D}\right)^{2/3} \quad (2)$$

We now calculate the structural weight of the UAV by using (3) given by Noth et al. (2008):

$$W_{af} = 0.3S^{1.2}AR^{1.3} \quad (3)$$

The weight of avionics is taken as 0.4Kg and the payload is taken as 3kg. Thus,

$$W = W_{af} + W_{bat} + W_{payload} + W_{avionics}$$

The power consumed by the avionics is taken as 20W and the nominal solar power is calculated as in section 2.1. The airfoil is chosen taking into consideration among other things the relative flatness of the top surface which makes the fabrication process more efficient. Also, as the cells will then be exposed to a near similar angle from the sun; the MPPT, which maximizes power from all the cells and not the individual cells, optimizes the system in a more uniform way, thereby also extracting maximum from each cell. The airfoil HN1036 is chosen for the middle

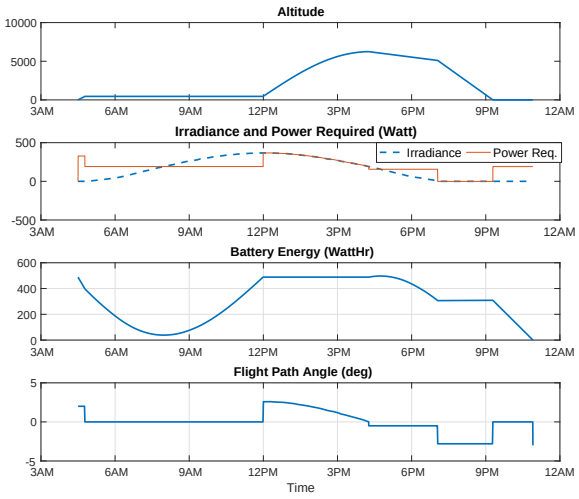

Fig. 3. 6DOF Simulation results

section with E197 on the tip sections. X-foil analysis showed that the combination generated higher $\frac{Cl^{3/2}}{Cd}$ than an individual airfoil. Assuming an AR and wing area, the 2D X-foil results were used to run the model and obtain new 3D finite wing values. The completed simulation gives total weight values which are then used to compute back the AR and S values and the procedure is repeated in iterative fashion until convergence to give final CL and CD values. The battery weight(W_{bat}) is calculated which is used to compute the required energy density. This is then compared to the state of the art value of available LiPo cells. The final results for the conceptual simulation are shown in Fig.2. As Li-Po batteries are commercially easily available, we use them as the main battery source. These have an energy density of 140Wh/Kg which gives us the wing-area of $2.04m^2$ and Aspect Ratio of 14. The total weight of the aircraft is predicted to be 17 kgs with structural weight at 9 kg.

3.2 Parametric values

A more detailed design analysis was carried by calculating the aerodynamic and stability derivatives as detailed in Nelson (1998) and Napolitano (2012) based on the aircraft parameters listed in table 2. Table 3 lists some of the aerodynamic and control derivatives which later were used in a 6-DOF offline simulator to calculate the optimum low power cruise speed and get an estimate of the power required by the system. The simulation results are shown in Fig. 3 .A stability analysis was also carried out to determine the location of the center of gravity to get a longitudinal stability margin of 15%.

4. MODEL REALIZATION

This section details the construction techniques and hardware used to build a prototype for the proposed SUAV.

4.1 Detailed design

Table 2 details the salient features of the proposed design. The CAD model, made for a detailed design study, is

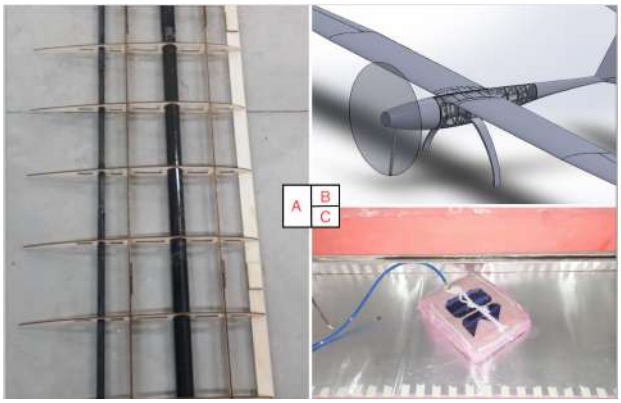

Fig. 4. Structural construction and encapsulation

shown in Fig. 4. Balsa was selected as the base material for construction owing to its light weight and flexibility. Ribs and formers were cut using an inhouse laser cutting machine. The internal structure is first coated with a 1.5mm balsa sheet which acts as a base for solar cells. Carbon-fiber rods were used to provide extra strength and necessary stiffness to the structure. The entire structure was reinforced with two layers of 120 gsm composite glass fiber which provided the required durability and smoothness. The wing internal structure can be seen in Fig. 4 A. Finally, the entire structure including the landing gear were designed and made using composite materials in order to adhere to the maximum weight constraints.

4.2 Solar cell encapsulation

A critical challenge in construction of a SUAV is the encapsulation of solar cells. A well designed and properly implemented encapsulation technique can increase the solar throughput and also minimize drag on the wing. There are two major reasons that make encapsulation extremely important for solar UAVs. Firstly, the overall performance of solar cells strictly depends upon the solar irradiance falling on the cells. The light falling on solar wafer has to pass through the encapsulation. Therefore the encapsulation must ensure the amount of light falling on wafer should be maximum for all incidence angles, intensities and for different frequencies in the spectrum of light. Secondly, the performance of solar cells should not decay with time and fatigue as well as the encapsulation must have sufficient mechanical strength. The performance of encapsulation can be studied in two major categories:

Optical performance: The reflection of light that accompanies the change of medium is minimum when the refractive indexes for both the mediums are as close as possible. The light falls on solar cells after traveling through three mediums: atmosphere, transparent sheet and adhesive. To ensure minimum reflection, and hence minimum loss of incident energy, the transparent sheet should have refractive index close to that of air and the adhesive should also have a similar refractive index to transparent sheet. Refractive index of a medium depends on the frequency of light also. Since the solar cells C60 generates power for frequency ranging from blue to red, the encapsulating material must also ensure maximum transparency for this spectrum range.

Part	Span (m)	Area (m^2)	Planform	Airfoil	Parameters	Value
Centre Section (2)	1.475	0.6785	Rectangular	HN1036	Total Wing Span	5.35 m
End Section (2)	1.2	0.468	Tapered	E-197	Wing Area	2.04 m^2
Horizontal Tail	1.35	0.418	Rectangular	E-297	Aspect Ratio	14
Vertical Tail	0.35	0.1158	Tapered	E-297	Max Wing Loading	7.84 kg/m^2

Table 2. Critical Design Parameters

Parameters	Value	Parameters	Value	Parameters	Value
CL_o	0.3	Cm_α	-1.926	Cy_p	-0.02
CL_α	5.03	$Cm_{\dot{\alpha}}$	-8.863	Cy_β	-0.049
$CL_{\dot{\alpha}}$	2.30	Cm_q	-26.8	$Cy_{\delta R}$	0.92
CL_q	6.98	Cl_β	-0.0045	Cn_β	0.178
$CL_{\delta E}$	0.309	$Cl_{\delta R}$	0.0185	Cn_r	-0.1
CD_0	0.01	Cl_p	-0.628	Cn_p	-0.02
CD_α	0.129	Cl_r	0.18	$Cn_{\delta A}$	0.11
Cm_o	0.03	$Cl_{\delta A}$	0.187	$Cn_{\delta R}$	0.06
$Cm_{\delta E}$	-1.18	Cy_r	0.031		

Table 3. Extended Design Parameters

Mechanical Performance The adhesive must ensure the safety of solar cells since the UAV exhibits significant vibrations due to the propulsion system. Also, the selection of encapsulating material be done carefully due to the presence of small fraction of ultraviolet irradiance in sunlight which may degrade the transparency of adhesive and transparent sheet with time. The dust present in the air and the air flow itself can also cause wear on the surface. The top surface therefore must ensure sufficient anti-wear property. The bubbles that appear during the encapsulation must be eliminated and lastly, the overall weight of encapsulation should not become too high as this will ultimately affect the endurance of the UAV.

For MARAAL prototype, we use two layers of 200gsm Ethylene-vinyl acetate(EVA). EVA is often used as a hot-melt-adhesive which has a property of becoming transparent after a short heating time. A layer of tedlar composite (tedlar polyester tedlar (TPT)) is used at the top to provide the necessary smoothness and weather resistance. As seen in Fig. 4 C, experiments were designed to validate the process of solar cell encapsulation. A state-of-art autoclave with a PID temperature control was designed with a provision for supporting vacuum bags. The pressure levels and temperature scheduling required for optimum finish are obtained after repetitive experiments on a wide variety of surfaces. Before installation, each of the solar cells is tested using a rated irradiance source installed within a reflective container as shown in Fig. 5 C. Only those cells that meet the minimum established standards are installed on the aircraft.

The solar cells are encapsulated using the following process: A wing section as shown in Fig 4 A is first coated with a sheet of balsa upon which two layers of 200gsm glass fiber were applied. After this first stage of curing, the solar cells are installed after electrical connections are established within all the cells. The solar cells are sandwiched between two layers of EVA which serve the dual purpose of holding the solar cells to the surface of the wing and also hold the TPT layer at the top. The entire arrangement is put inside a vacuum bag after being shielded by a breathing cloth. Vacuum is applied to achieve a pressure of 7.5 inHg. The setup is heated using the custom made autoclave. The setup is taken to 95°C in steps of 10 degrees per 5 min

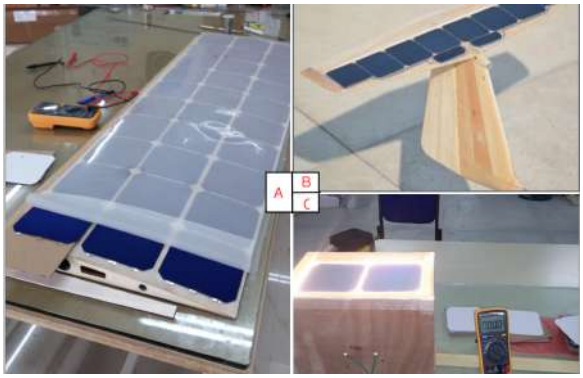

Fig. 5. Installation and testing of solar cells

after which the temperature is held constant at 95°C for 2 min. The setup is subsequently cooled down till room temperature and tested for any abnormalities. Solar cells are installed on the wings and the tail plane as shown in Figs. 5 A and B respectively.

4.3 Electronics and power

As the aircraft cannot be flown for extended amount of time and beyond line of sight using tele-operation, a commercially available open source autopilot(See PixhawkMeier et al. (2011)) is used with the PX4 flight stack. The entire circuit plan is as shown in Fig 6.The SUAV uses a KDE Direct 8518XF120 BLDC motor with a 30.5×9.7ẗriple blade propeller. For surveillance purposes, a 2-axis brushless gimbal was designed with vibration dampening. Gimbal stabilization was provided using an open source Storm32 brushless gimbal controller board by OlliW (2013). The gimbal utilizes brushless motors as against to servos as gimbal motors offer smoother control and an unrestricted 360° rotation. The camera used was a Logitech C270. Both the telemetry and camera feed were supplied to a high performance computer which was connected to a long range radio module. The module transmitted the images and telemetry to a ground control station with a latency of less than a second using the gstreamer package Team (2013). The UAV communication module has a diversity ominidirectional and patch antenna structure which was range tested to a distance of 10kms.

5. FLIGHT TESTS

Maiden test flight for MARAAL was conducted on 1st April 2017 which was a solely radio controlled flight[https://www.youtube.com/watch?v=ysHjxsj-ha0]. All the flight tests took place at airstrip within IIT Kanpur campus. In subsequent flights the autopilot was tested and parameters tuned to achieve optimum path following performance and minimum power velocity tracking. Flight test results for a 8h 30min flight conducted on 13th April 2017 are shown. The aircraft took off at 9:30 am IST

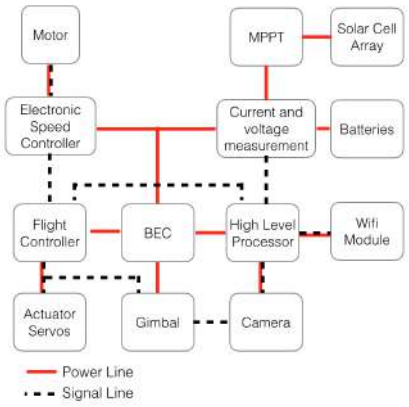

Fig. 6. Onboard Circuitry

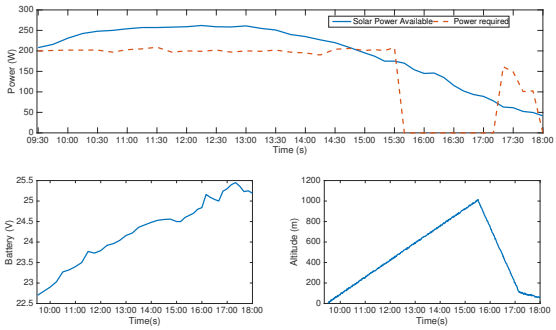

Fig. 7. Flight Test results

with near-depleted batteries and was commanded to climb at a constant climb rate of 0.05m/s. The optimum low power velocity was identified at 23 m/s which was given as command input to the autopilot. The power consumed by the system, generated by the solar cells and the battery charging status are shown in Fig. 7. At around 3:30pm, the generated power became less than the power required by the system. At this point the throttle was cut-off and the aircraft was commanded to glide maintaining a sink rate of 0.15m/s. The power generated during this time was used to keep charging the batteries. This was arrested at 100m altitude where a lower sink rate with throttle was commanded to charge the batteries to the full before landing. The aircraft successfully landed at 6 pm IST with a fully charged battery. The altitude graph is shown in Fig. 7. Combined with the 4 hour endurance on a fully-saturated battery validated in a separate flight, the total endurance can potentially be 16 hours in April.

6. CONCLUSION

The design, prototyping and flight testing of a 5.35m LALE-SUAV for surveillance in a sub-tropical climate is presented.In-flight measurements for a 8h 30min flight on 13th April are presented which confirm the expected 16hr endurance. All the goals of the study are met by (A) using a detailed conceptual approach towards designing by mathematically modelling the constraints and using a 6DOF flight simulation on the derived parameters; and (B) by improvements in the encapsulation process that ensures a smooth flow over the wing.Future work involves more involved flight tests with autonomous mission planning using a maximum energy-efficient approach.

REFERENCES

Berni, J.A., Zarco-Tejada, P.J., Suárez, L., and Fereres, E. (2009). Thermal and narrowband multispectral remote sensing for vegetation monitoring from an unmanned aerial vehicle. *IEEE Transactions on Geoscience and Remote Sensing*, 47(3), 722–738.

Cocconi, A. (2005). Ac propulsions solar electric powered solong uav. *AC Propulsion, Tech. Rep.*

Colella, N.J. and Wenneker, G.S. (1996). Pathfinder. developing a solar rechargeable aircraft. *IEEE Potentials*, 15(1), 18–23.

Duffie, J.A. and Beckman, W.A. (2013). *Solar engineering of thermal processes*. John Wiley & Sons.

Dunbabin, M. and Marques, L. (2012). Robots for environmental monitoring: Significant advancements and applications. *IEEE Robotics & Automation Magazine*, 19(1), 24–39.

Goodrich, M.A., Morse, B.S., Gerhardt, D., Cooper, J.L., Quigley, M., Adams, J.A., and Humphrey, C. (2008). Supporting wilderness search and rescue using a camera-equipped mini uav. *Journal of Field Robotics*, 25(1-2), 89–110.

Hottel, H.C. (1976). A simple model for estimating the transmittance of direct solar radiation through clear atmospheres. *Solar Energy*, 18(2), 129–134.

Meier, L., Tanskanen, P., Fraundorfer, F., and Pollefeys, M. (2011). Pixhawk: A system for autonomous flight using onboard computer vision. In *Robotics and automation (ICRA), 2011 IEEE international conference on*, 2992–2997. IEEE.

Napolitano, M.R. (2012). *Aircraft dynamics: From modeling to simulation*. J. Wiley.

Nelson, R.C. (1998). *Flight stability and automatic control*, volume 2. WCB/McGraw Hill New York.

Noth, A. et al. (2008). *Design of solar powered airplanes for continuous flight*. Ph.D. thesis.

Oettershagen, P., Melzer, A., Mantel, T., Rudin, K., Lotz, R., Siebenmann, D., Leutenegger, S., Alexis, K., and Siegwart, R. (2015). A solar-powered hand-launchable uav for low-altitude multi-day continuous flight. In *Robotics and Automation (ICRA), 2015 IEEE International Conference on*, 3986–3993. IEEE.

OlliW (2013). Storm32-brushless gimbal controller. `http://www.olliw.eu/2013/storm32bgc/`. Online, Accessed: 23rd Aug 2017.

Ross, H. (2008). Fly around the world with a solar powered airplane. *Power*, 1(8), 1–9.

Sai, L., Wei, Z., and Xueren, W. (2017). The development status and key technologies of solar powered unmanned air vehicle. In *IOP Conference Series: Materials Science and Engineering*, volume 187, 012011. IOP Publishing.

Team, G. (2013). Gstreamer: open source multimedia framework.

Wilkins, G., Fourie, D., and Meyer, J. (2009). Critical design parameters for a low altitude long endurance solar powered uav. In *AFRICON, 2009. AFRICON'09.*, 1–6. IEEE.

Zhang, C. and Kovacs, J.M. (2012). The application of small unmanned aerial systems for precision agriculture: a review. *Precision agriculture*, 13(6), 693–712.